

Transmission Characteristics of the Dynamic Response to Episodic Forcing in the Warm Pool Regions of the Tropical Oceans

Peter J. WEBSTER, Hai-Ru CHANG and Chidong ZHANG

*Department of Meteorology
The Pennsylvania State University
University Park, PA, 16802 - U.S.A.*

ABSTRACT

In the warm pool region of the Pacific Ocean, the strongest and most intense convective heating in the global atmosphere occurs. The form of the heating is episodic, lasting for periods of days with scales of order 2-3000 km generating a spectrum of waves. The modes that are excited range from the mixed Rossby-gravity wave to the equatorially trapped Rossby and Kelvin waves. However, these transient modes are produced in a complex basic state which includes both horizontal and vertical shear and horizontal stretching deformation. To determine how they extend their influence from the warm pool region to other, more remote areas of the globe, we are required to reconsider the basic theory of equatorial waves in basic states of different signs, latitudinal shear and longitudinal stretching deformation. It is shown that the waves are extremely sensitive to each of these factors. Depending on the sign of the basic state, the waves "swell" poleward differentially. In particular, the turning latitudes of modes in the equatorial westerlies is about twice that for the equatorial easterlies; 15° compared to 30°-40° for observed values of the basic flow. The longitudinal stretching deformation causes regions of energy accumulation within the equatorial westerlies. Modes reach the accumulation zone in different directions depending on their scale. The short-scale end of the excited wave packet, which has initial weak easterly group speeds and stronger eastward Doppler-shifted group speeds, approaches the westerlies from the west. Through the modifications that the wave must undergo from conservation principals, the Doppler-shifted group speed approaches zero in the region of negative stretching deformation. The long-wave end of the packet, with westward group speeds, approaches the westerlies from the east where, for the same conservation reasons, the Doppler-shifted group speed also approaches zero. In the equatorial westerlies, the accumulated wave energy "swell" to higher latitudes as the turning latitudes of the modes modify in the westerly wind regime. In this manner, corridors through which energy passes from the convective regions of the tropics to higher latitudes are created.

1. Introduction

The warm pool regions of the tropical oceans contain the most vigorous convection on the globe. The largest warm pool exists between the western Pacific Ocean and the eastern Indian Ocean, spanning the Indonesian Archipelago. If sea surface temperatures greater than 28°C are used as a criterion, the West Pacific-East Indian Ocean warm pool covers about one eighth of the surface area of the globe. Within the heart of the warm pool, annual precipitation exceeds 4 m. The convection associated with the precipitation appears to be highly organized with space and time scales of greater than 2-3000 km and of the order of a week or greater, respectively (Nakazawa, 1988, Lau et al, 1988). Observations and models suggest that the intense and impulsive convection may promote the excitation of transient modes. Other studies (e.g., Lau and Chan, 1985) suggest that these transients exert considerable influence on the extratropics and that the midlatitude response is often phase locked irrespective of the phase of the equatorial forcing.



F30237

Despite the evidence of the existence of strong forcing in the warm pool regions and the observations of energy radiating away from the energy source both along the equator and into the mid latitudes, there exists a relative ignorance of how the influence is transmitted globally. Part of the problem is that the forcing takes place in an extremely complicated basic or background state. The basic flow, forced by the slowly varying heating associated with the sea surface temperature (SST) field contains both horizontal and vertical shear and horizontal stretching deformation (Webster and Chang, 1988). Figure 1a provides a schematic diagram of the near-equatorial background flow in the longitude-height plane at extremes of the Southern Oscillation (Webster, 1987). Figure 1b shows the character of the boreal winter upper tropospheric flow. Elementary theory of equatorial modes is not applicable to such complicated basic states. Thus, to understand wave transmission in complicated basic states, it is necessary to examine existing theory.

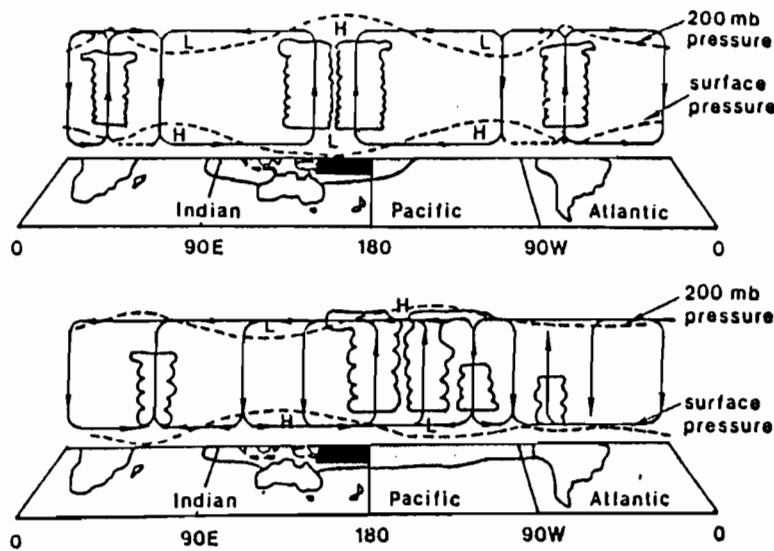


FIG.1. Schematic diagram of the zonal circulations along the equator for La Nina (upper panel) and El Nino (lower panel). Clouds represent regions of maximum mean convection. Stippled regions indicate sea surface temperatures warmer than 28°C. Waves represent genesis regions of equatorial transients. (after Webster, 1983)

Equatorial dynamics has a relatively short history in the atmospheric sciences. It was not until the late 1960's that a series of observational and theoretical studies provided a new basis for understanding the elementary physics of the large-scale tropical atmospheric circulation. Foremost in these studies was Matsuno (1966) which provided new and enlightening perspectives. It showed that classes of very large-scale modes existed which possessed a mix of divergent and rotational characteristics that were trapped about the equator. Matsuno's study, which used a β plane formulation in a quiescent fluid, showed that there were a number of mode families that were equatorially trapped. These were the Rossby wave, the eastward and westward propagating mixed Rossby-gravity and gravity modes and the Kelvin mode. Later, Longuet-Higgins (1968) was able to show that Matsuno's solutions were asymptotics of general spherical modes as the parameter ($4\Omega^2 a^2 / gh$) becomes large. The dispersion curves for modes with $h=300$ m are shown in Fig. 2.

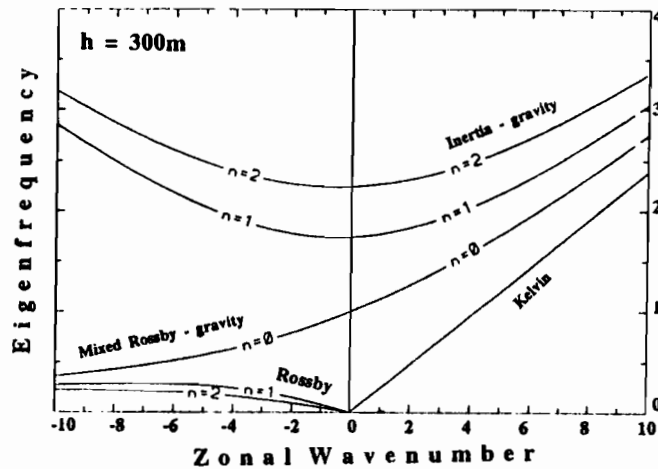


FIG.2. Dispersion curves of equatorially trapped modes for an $h=300$ m fluid. (Zhang and Webster, 1989).

A number of studies considered the properties of equatorial modes in simple non-zero basic states. As the complexity of the states increased so did the applicability of the theory to the solution of practical physical problems. Using zonally symmetric basic states (i.e., $U=U(y)$), Webster (1972, 1973) and Gill (1980) suggested that the mean structure of the tropics could be thought of as the response of equatorially trapped modes to stationary forcing produced by the latent heat release associated with the mode itself and the sea-surface temperature distribution. Opsteegh and Van den Dool (1980), Hoskins and Karoly (1981), Webster (1981, 1982), among others, have speculated that anomalous forcing along the equator within simple $U(y)$ flows produce propagating wave trains. Thence, the theory continues, the global climate is perturbed during periods of anomalous forcing such as El Niño. Figure 3 shows the boreal winter and summer anomalous atmospheric responses relative to anomalous equatorial heating akin to the difference between latent heating during warm events and more normal times in the Pacific Ocean.

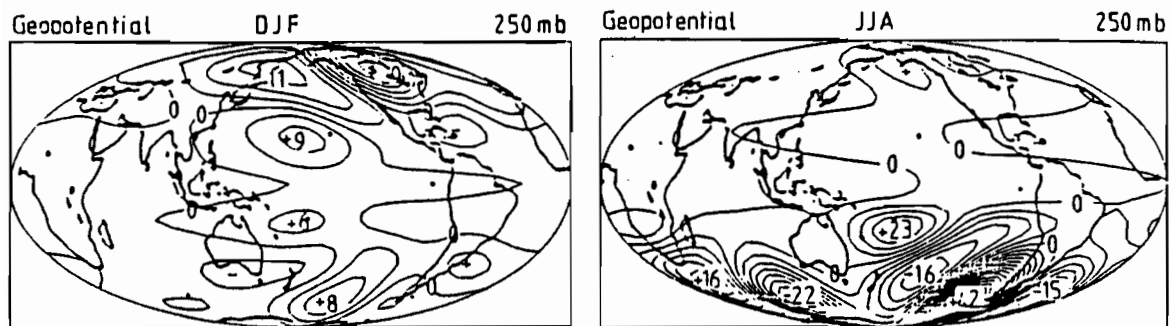


FIG.3. The 250 mb geopotential response of a zonally symmetric boreal winter (right panel) and summer (left panel) zonal wind distribution to a steady heat source placed in the central Pacific Ocean. (Webster, 1982).

Whereas the steady state models predict many features of the observed anomalous behavior, including maximum perturbation of the winter hemisphere, it has become apparent that the physical basis of the system is too simplistic. In other words, the steady state theory suffers from a number of problems. First, if the forcing moves in location, the pattern must also move. Observations show that warm events differ markedly in form and intensity. Both observations and numerical modeling show that the

global influence pattern is more robust and is relatively invariant in its' position to the shape and magnitude of the forcing function. Also, a steady state model ignores the transient nature of the atmosphere. The mean annual heating is comprised of a series of strong impulsive events. Thus, unless the state model can somehow mimic the aggregate of these transients, one can expect differences between the steady state solutions and the mean atmospheric response. Finally, the excitation of the Rossby wave train from within the easterlies, which the steady state models predict, requires either that the forcing extends to the westerlies or that nonlinear effects are important (Sardeshmukh and Hoskins, 1988).

Besides impacting the circulation of the higher latitudes, equatorial forcing also produces a considerable perturbation to the mean flow at low latitudes, at least in its' aggregate effect. The combination of forced equatorially trapped Rossby and Kelvin modes produces regions of perturbation easterlies and westerlies along the equator. The perturbations are sufficiently strong to produce regions of net westerlies in the tropical upper troposphere which are apparent for most of the year over the eastern Pacific and Atlantic Oceans. Thus, in reality, the basic flow, at least as far as the transients are concerned, has a strong three-dimensionality such that $U=U(x,y,z)$.

2. Magnitude, scale and duration of episodic convective heating in the tropical regions: the case for strong episodic forcing.

Outgoing longwave radiation (OLR) has been used as a surrogate for precipitation for a number of years (Arkin and Meisner, 1987). Figures 4a and b show the boreal summer (upper panel) and winter (lower) OLR distributions in the equatorial strip. Concentrating on values of $OLR < 240 \text{ W.m}^{-2}$, we note that there are three major minima: over equatorial Africa and the central Americas and, the largest, over the eastern Indian Ocean and western Pacific Ocean which spans Indonesia. All three centers show an annual cycle with a migration towards the summer hemisphere. At all times of the year, a large minima remains in the western Pacific Ocean. By extension (Arkin and Meisner, 1987), we can infer that intensive precipitation occurs at all times of the year. Heating functions derived from such precipitation distributions have been used to drive steady state circulation models in an attempt to model the mean tropical circulation (e.g., Webster, 1972¹, 1981, 1982, Opsteegh and van den Dool, 1980, Hoskins and Karoly, 1981). To a large degree, these models were able to simulate and explain the strong three-dimensional character of the mean tropical flow such as that shown in Figs. 1 and 3.

Assessing the magnitude of the western Pacific Ocean precipitation with accuracy is rather difficult. Figure 5 provides an estimate of the Pacific Ocean annual precipitation using island data (Taylor, 1972). The analysis shows a broad region of precipitation in the western Pacific Ocean of order of 4-5 m and an elongated maximum north of the equator. The first feature appears to be associated with the warm pool region of the western Pacific Ocean (i.e., surface temperature $> 28^{\circ}\text{C}$) and the second with the ITCZ. Whereas it is very difficult to determine absolutely if the magnitudes of Taylor's analysis is representative away from the islands, the satellite estimates of Motell and Weare (1987) indicate that, at least, the patterns of precipitation are reasonable. The task is to determine the heating associated with this precipitation, with the transient

1. Actually, in Webster (1972) brightness data was used to infer convective cloudiness and, thence, precipitation and latent heating. Visible brightness data alone, however, provides an ambiguous estimate of precipitation as both stratus layers and desert areas are also bright. Thus, a certain degree of subjectivness was used.

components of the mean heating and the scale of the divergence associated with them. Measures of the associated divergence are necessary as these are used to drive the free surface barotropic model.

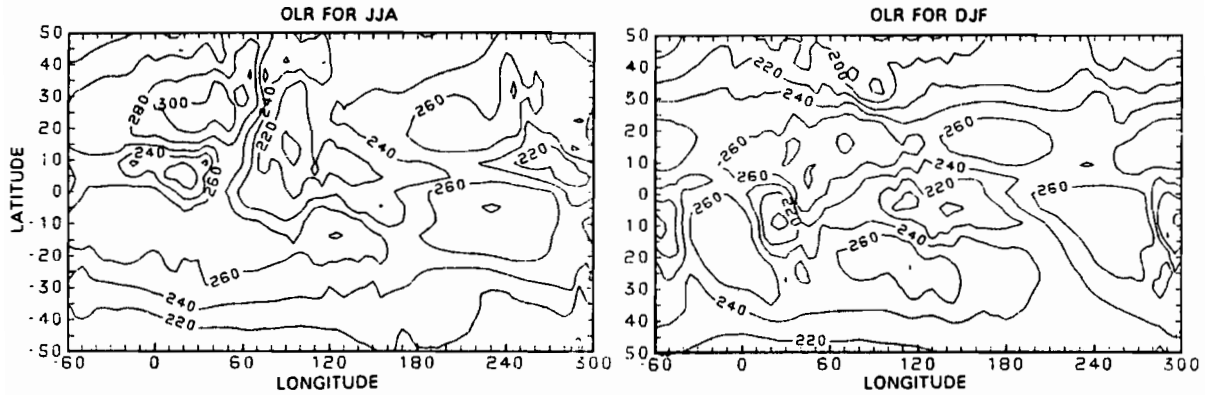


FIG.4. The mean outgoing longwave radiation observed from satellite for (a), the boreal summer and (b), the boreal winter. Units $W.m^{-2}$.

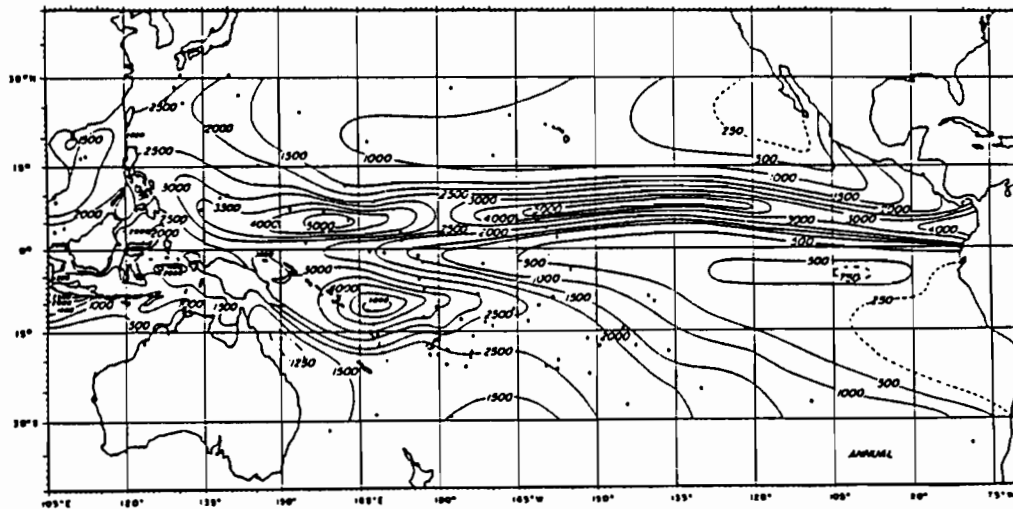


FIG.5. Estimate of the mean annual precipitation in the Pacific Ocean using ocean island rainfall data. (Taylor, 1972).

a. Mean heating rates in the warm pool regions.

Using an estimate of 3.5 m as the annual precipitation over the western Pacific Ocean from Fig. 5, the equivalent heating rate per unit mass of air can be calculated to be about $2^{\circ}C \text{ day}^{-1}$. An estimate of the average divergence associated with the heating can be calculated by assuming a rough balance between diabatic heating and the ensuing adiabatic ascent (e.g. Webster, 1983). For a simple vertical structure extending through the entire tropical troposphere with a maximum in the middle troposphere, the resulting low level convergence associated with the $2^{\circ}C \text{ day}^{-1}$; heating is $0.6 \times 10^{-6} \text{ s}^{-1}$.

We can check this estimate with divergences obtained from the European Centre for Medium Range Weather Forecasting/World Meteorological Organization (ECMWF/WMO) Global Analysis Data Sets. The data sets consist of six physical variables at seven standard pressure levels listed twice per day (12 and 00 Z) on a $2.5 \times 2.5^{\circ}$ latitude-longitude grid. Figure 6 shows the annual average (upper panel) and a series of 2-month averages (lower panels) of the horizontal divergence at 850 mb (left column)

and 200 mb (right column), respectively, along the equator between 90°E and 150°W for 1980. At 850 mb, the region between 140°E and 180°E shows persistent convergence (shaded) of magnitudes of -1 to $-2 \times 10^{-6} \text{ s}^{-1}$. The region of convergence spans the maritime continent of Indonesia and the western Pacific Ocean warm pool. During the boreal summer, substantial convergence exists in the Indian Ocean. Very strong upper level divergence (shaded) is apparent over the Indonesian West Pacific region at all times of the year. Clearly, from Figure 6, it is obvious that there is strong heating in the mean between about 140°E and 180°E. However, it does not show the spatial and temporal scales of the higher frequency organized divergence which aggregates to provide the mean divergence fields.

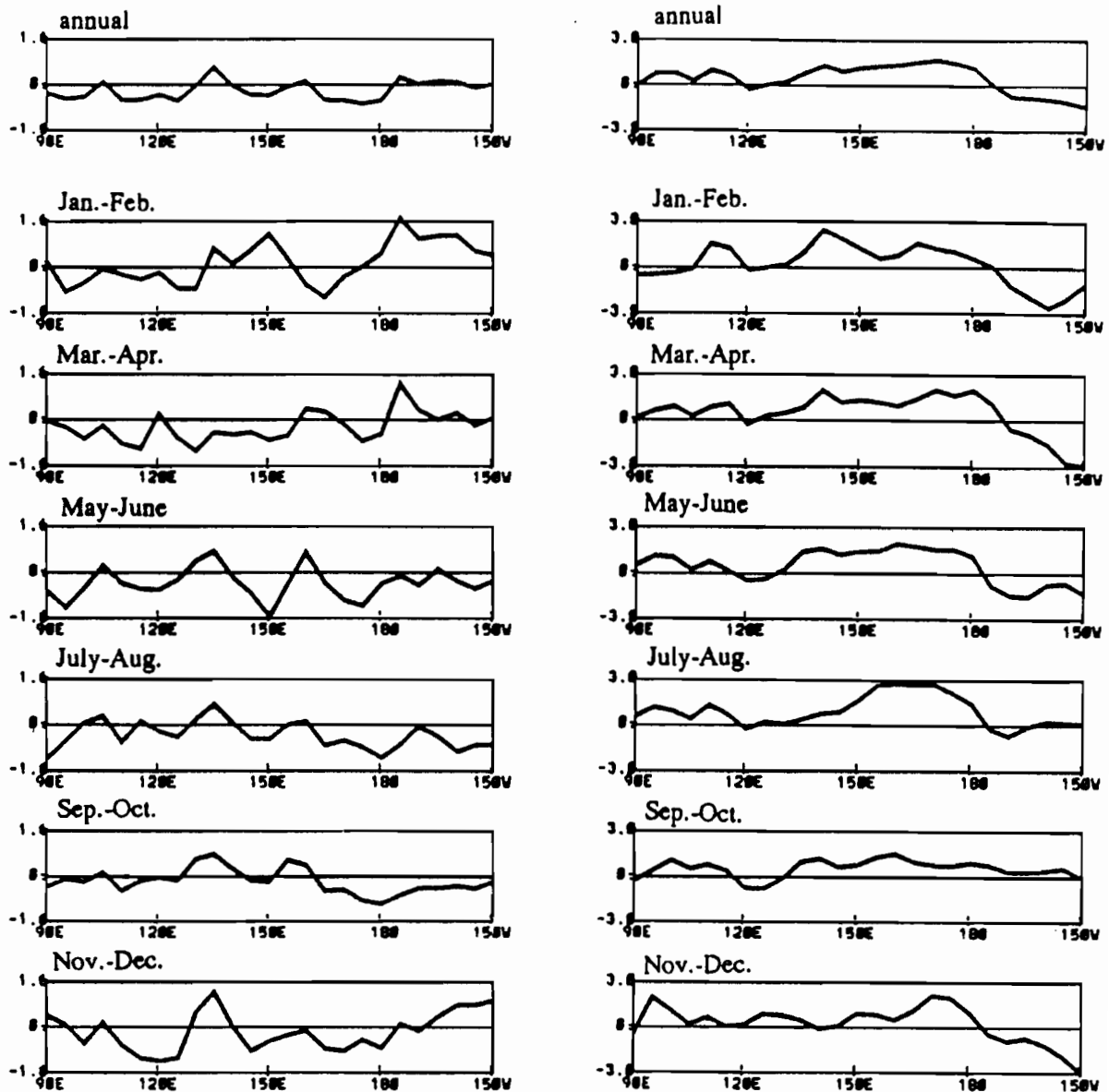


FIG.6. The horizontal divergence at 850 mb (left column) and 200 mb (right column). The annual average is shown in the two top panels. Bi-monthly averages are shown in the lower panels. Units 10^{-6} s^{-1} . (Chang and Webster, 1989).

b. Low frequency variations in the heating rates in the warm pool regions.

Figures 7a-d show longitude time sections along the equator of divergence (units 10^{-6} s^{-1} between 90°E and 150°W). Each panel shows two month segments. Regions of convergence are shaded. By comparing these sections with Figure 6, we can see that the moderate values of net convergence are replaced with large, low frequency periods of divergence. Indeed, values often exceed $-5 \times 10^{-6} \text{ s}^{-1}$ for periods of days and scales of order 3-5000 km. That is, the annual divergence pattern over the warm pool regions is comprised of a series of strong episodic events. Such events have been referred to as "super clusters" by Nakazawa (1988) and Lau et al. (1989). We show here that the "super clusters" are associated with convergence on an order of magnitude greater than the annual mean. Thus, the heating rates associated with the episodic events range from 10° to $20^{\circ}\text{C}\cdot\text{day}^{-1}$ and have typical periods of days and longitude scales of 3-5000 km.

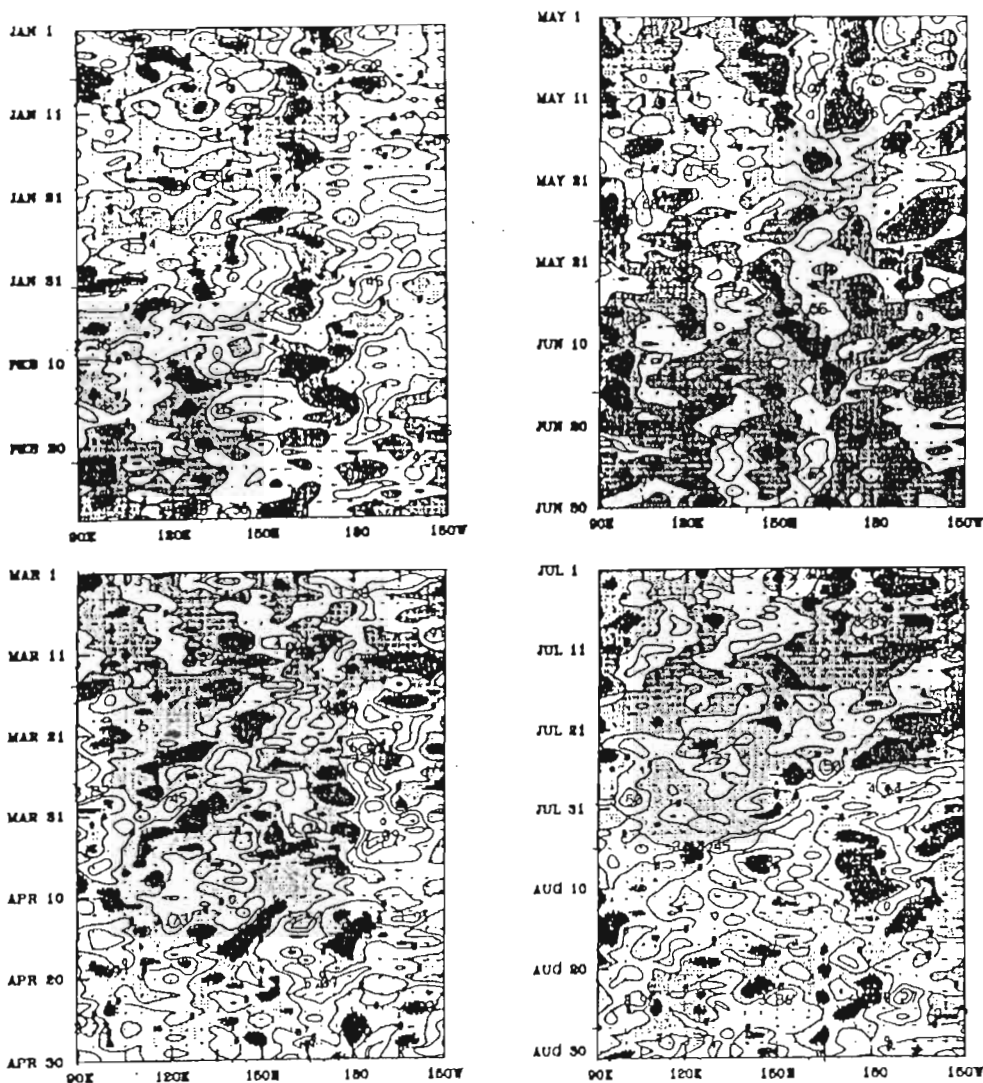


FIG.7. Time-longitude sections of the 850 mb divergence fields plotted between 90°E and 150°W . The sections show the substructure of the first four mean bi-monthly lower tropospheric divergence fields shown in the left column of Fig. 3. Shaded areas denote convergence. Heavier shading indicates convergence $> 2 \times 10^{-1} \text{ s}^{-1}$ and the heaviest shading $> 4 \times 10^{-1} \text{ s}^{-1}$. Note the prolonged periods of convergence occurring along broad regions along the equator.

c. Formulation of a realistic transient tropical heating function.

If a free surface barotropic model (see Webster and Chang, 1988) is used to model the tropical atmosphere, a divergence function acts as a mass source-sink function. This is equivalent to heating in a baroclinic model. With the divergence fields displayed in Fig. 7 in mind, we define an appropriate transient forcing function as:

$$m(x,y,t) = E J(x,y) \tau(t) \quad (1)$$

where E is the mass source sink amplitude function J and τ are the spatial and temporal functions

$$J(x,y) = \exp(-|x-x_0|/2) \cdot \exp(-|y-y_0|^2/4) \quad (2)$$

and

$$\tau(t) = (t^3 / 2\delta^3) \exp(-t/\delta) \quad (3)$$

Figure 8a shows the variation of the amplitude function with respect to time (i.e). The right hand scale shows the equivalent divergence and heating rates associated with the episodic forcing. Figure 8b plots the horizontal distribution function $J(x,y)$. With an appropriate equivalent heating function defined, we are ready to study the basic modes in more realistic basic flows.

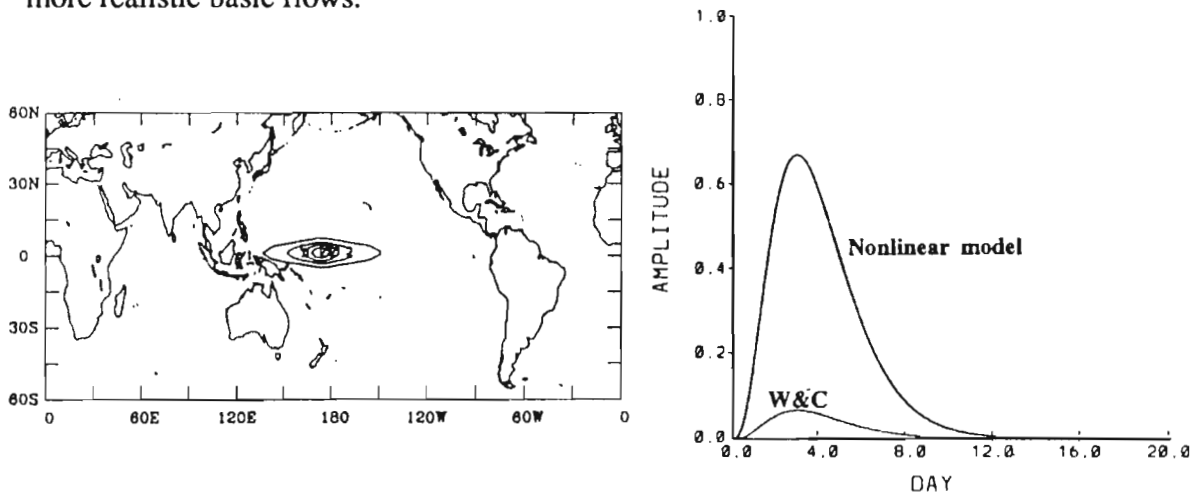


FIG.8. (a) The time evolution of the forcing function defined in (1). Units: 10^{-1} s^{-1} . (b) The spatial distribution of the forcing is normalized to a value of 5.

3. New concepts of equatorial waves: consideration of more realistic basic flows.

a. Influence of the sign of the basic state and latitudinal shear on the structure of equatorial transients.

On a rotating sphere, the longitudinal phase and group speed of a rotational wave are determined by the scale of the mode, the rate of rotation, and the basic state within which the mode resides. That is, the distribution of the mode is determined by the local ambient potential vorticity gradient (Zhang and Webster, 1989: Z&W) inherent in the basic state. In the tropics, the result is a longitudinal cell (often referred to as the Walker Circulation) which produces variations of the zonal velocity along the equator (Webster, 1983). These regional westerlies may then be further enhanced by the equatorward transport of westerly momentum through the "westerly duct" by extratropical eddies (Webster and Holton, 1982).

Figure 9 shows the observed 200 mb zonal velocity component for the boreal winter. Note that along the equator, distinct regions of easterly and westerly winds exist, ranging roughly from -15 m.s^{-1} to 20 m.s^{-1} . The eastern hemisphere is characterized by very strong latitudinal shear and easterlies along the equator. The western hemisphere, on the other hand, possesses much weaker shear and, in general, also produces westerlies along the equator. For the boreal summer, easterlies extend around most of the equator. However, the longitudinal structure of the first derivative of the zonal wind component (U_x) remains much the same.

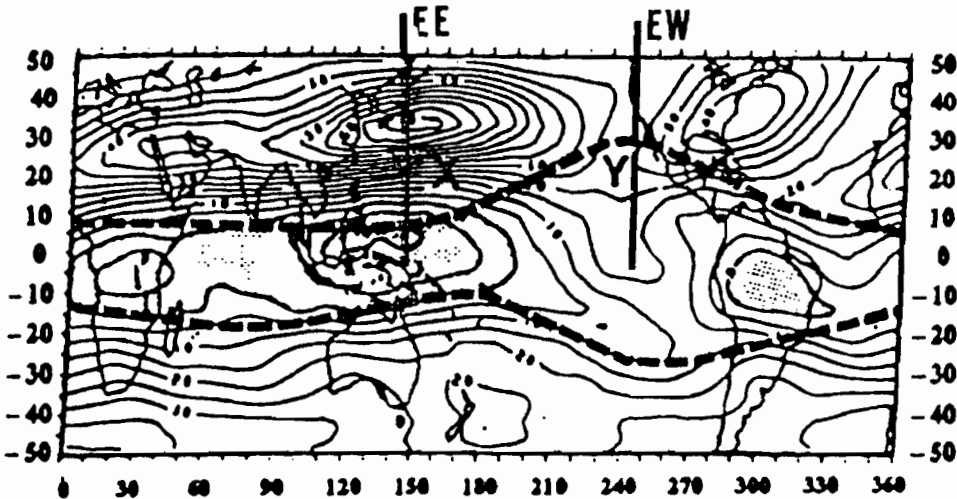


FIG.9. The mean 200 mb zonal wind field. Shaded areas denote easterlies. The lines EE and WE show typical shears through the eastern and western hemispheres. The dashed line refers to the turning latitude of a $k=3, n=1$ Rossby wave. (Zhang and Webster, 1989).

Figure 10 shows the perturbation zonal velocity component of the $n=2, k=3$ equatorial Rossby wave on an equatorial β plane for constant basic states of $U=+10, 0$ and -10 m.s^{-1} (Z&W). Note that in the westerly regime, the mode extends considerably more poleward. Z&W show that the impact of the variation of the basic state increases with increasing k and n . Figure 11 depicts contours of the turning latitudes of the modes as functions of k and n for $U=+10$ and -10 m.s^{-1} . Clearly, when the basic flow is westerly, the equatorial trapped mode encroaches extensively into higher latitudes as k and n increase. In Section 3(e), we will see that this encroachment or swelling property of the equatorially trapped mode is rather important, especially in regions where the stretching deformation is substantial. There, the scale of the transients must change.

ROSSBY

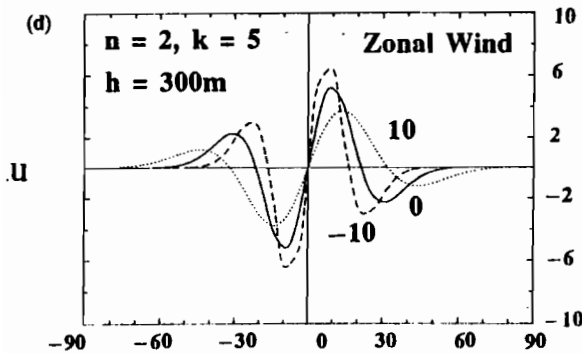


FIG.10. The latitudinal structure of the perturbation zonal velocity of the $n=2, k=3$ Rossby mode for background basic states of $U= -10, 0,$ and 10 m.s^{-1} .

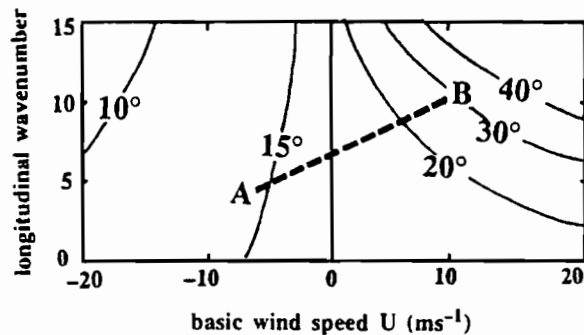


FIG.11. Contours of the turning latitude of the Rossby modes as a function of U as a function of k for $n=1$.

Figure 12 shows the zonal velocity structure of the equatorial Rossby wave in the shear flows EE (shear flow with equatorial easterlies) and EW (equatorial westerlies) from Fig. 8. Very little difference exists between the two cases and each is less equatorially trapped than in a basic state at rest. Z&W use potential vorticity arguments to show that the structure variation in different basic states is consistent with the variation restoring force associated with the ambient potential vorticity latitudinal gradient.

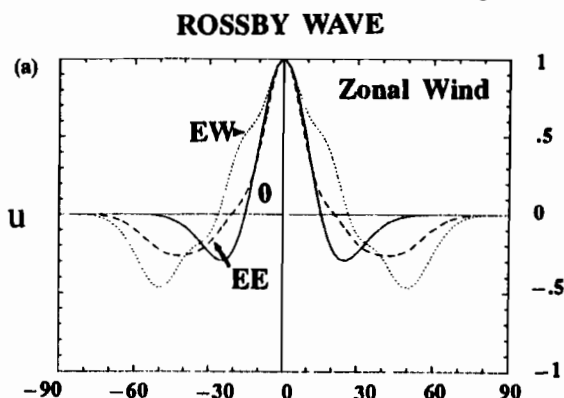


FIG.12. The perturbation zonal velocity component of the equatorial Rossby wave in shear flows EE and EW of Fig. 9. From Zhang and Webster (1989).

b. Extratropical influences on the tropics.

Most studies have concentrated on the horizontal variation of the low frequency basic flow, i.e., $U=U(x,y)$. Using a barotropic model, Karoly (1983) showed that the ray paths of equatorial modes were greatly affected by the horizontal variability of the basic state. However, being a barotropic model, Karoly could not consider equatorially trapped modes as such modes do not exist in a barotropic fluid (see Webster and Chang, 1989: W&C). With a free surface barotropic model, and, thus, a divergent system, Webster and Holton (1982) were able to show that regions of westerlies, which they termed the "westerly duct", acted as wave guides or conduits across the equator between the westerlies of the extratropics of each hemisphere. Thus, in general, the equatorial regions may be thought of as being much more "porous"; to extratropical influence than initially thought, for example, by Charney (1969) and Mak (1969). In addition, Webster and Holton found evidence that the extratropical forcing also produced trapped modes about the equator, although they could not explain the result. Figure 13 shows the response of the Webster-Holton model to forcing located at different longitudes in the extratropics.

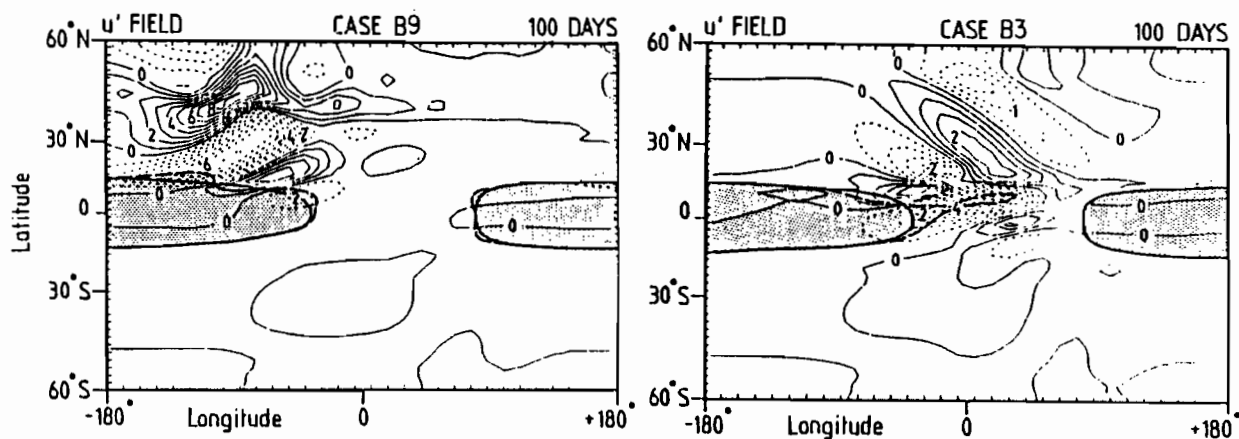


FIG.13. Responses of a $U(x,y)$ basic state to forcing located at different regions in the extratropics. Shaded region denotes easterlies. From Webster and Holton (1982).

c. Equatorial transient wave energy accumulation:

The low frequency standing waves along the equator which produce the three dimensional basic state provide a very complicated flow through which equatorially trapped transients must propagate. Indeed, the study of free and forced modes within a more realistic basic state has revealed a much richer structure than was previously thought to exist.

In a series of recent studies (Frederiksen and Webster, 1987; Webster and Chang, 1988; W&C; and Zhang and Webster, 1989), the importance of the slowly evolving background flow (or at least the horizontal part of it, $U(x,y)$) of the tropical atmosphere on transient tropical structures, has been studied at length. W&C showed that an equatorially trapped Rossby mode propagating along the equator is severely modified by the longitudinal variation of the basic flow. Specifically, they showed that regions where $U_x < 0$ (note the regions to the east of the equatorial westerlies in Fig. 9), were regions of energy accumulation. Basically, transient equatorially trapped modes would tend to accumulate in this region for a number of fundamental reasons. A major deduction of the W&C study was that, irrespective of where excitation occurred along the equator, ultimately, forced modes would become trapped in the regions of negative stretching deformation.

The physical basis for the arguments of W&C are rather simple. The combination of the strength of the basic flow and the stretching deformation and the group speeds of equatorially trapped modes allow for the possibility of the Doppler-shifted group speed C_{gd} to approach zero. Figure 14 shows the variation of the group and phase speeds as a function of the equivalent depth. For small k , the velocities are generally easterly. The shaded region denotes the regime within which group and phase speeds are equal and opposite the observed westerly winds shown in Figure 9. That is, zero Doppler-shifted group speeds are possible. Note that for larger values of k , the group speeds are westerly. Thus, it would seem that for these smaller scale modes, Doppler-shifted group zeros are not possible. However, it will be shown (see d below) that the equatorial westerlies provide a wave attractor region such that in the observed parameter range, produce Doppler-shifted group speed zeros for all scales.

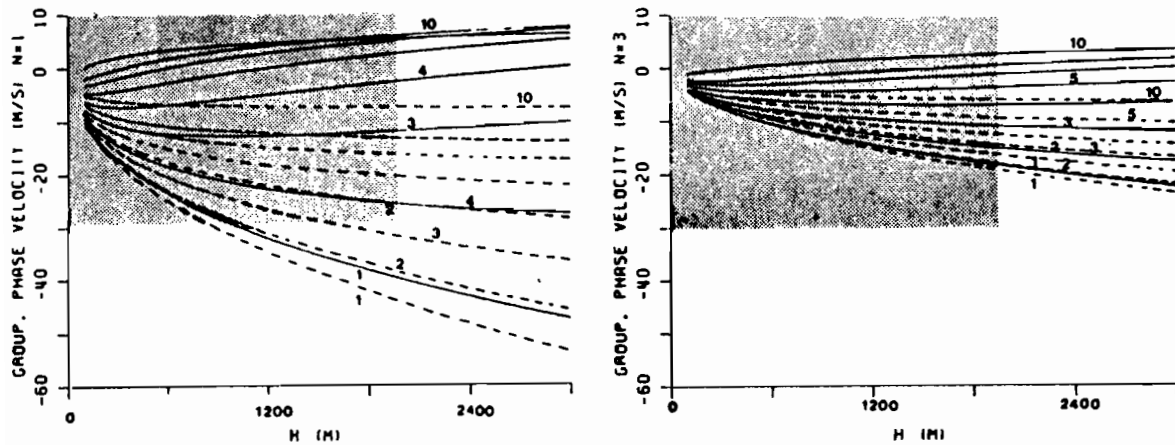


FIG.14. Variation of the group (solid lines) and phase (dashed) speeds for various k . Shaded region denotes the observed parameter range of the westerly winds and the vertical scale. From Webster and Chang (1988).

It turns out, however, that the situation is far more complicated than would seem by merely considering the Doppler-shifted characteristics of a mode in a variable basic state. W&C show that along a ray within a flow where $U=U(x)$, the horizontal wave

number must change in order to conserve the Doppler-shifted frequency $\omega_d = (\omega - kU)$ if the basic flow is time invariant. For a trapped Rossby mode, the rate of change of k along a ray is given by:

$$dk/dt = \partial k/\partial t + (U + \partial\omega/\partial k) \partial k/\partial x = -k dU/dx \quad (4)$$

Thus, if $U_x < 0$, a propagating mode must increase its' scale (k larger) and, conversely, if $U_x > 0$, the mode must increase its' scale (k smaller). Consistent arguments relating to the wave action flux show that:

$$\partial\varepsilon/\partial t + C_{gd} \partial\varepsilon/\partial x = -\varepsilon dU/dx \quad (5)$$

where ε is the wave energy density. Thus, where $U_x < 0$, there is a convergence of wave energy and vice versa. W&C conclude that, for the observed parameter range suggested in Figure 9, there should be considerable modification of the equatorial wave characteristics by the longitudinal variation of the basic flow.

W&C did note that if the scale of the initial westward propagating transient was sufficiently large, it would be possible for the mode to pass through the negative stretching deformation "trap". Although the mode would suffer under distribution during its' passage through the zonally varying flow, it could, nevertheless, be free to continue its' westward propagation. However, they concluded that, in the real atmosphere, the strength of the basic flow is sufficiently strong to trap all but the gravest transient mode. Chang and Webster (1989) were able to show that the accumulation process was sufficiently robust to transcend linearity into the non-linear regime.

With the W&C hypothesis of accumulation and Z&W mode sensitivities to the form of the basic state in mind, it is possible to anticipate the total impact on a mode propagating through a basic state which possesses substantial stretching deformation along a ray.

d. The concept of the "westerly attractor".

W&C concentrated on the long wave end of the spectrum where waves possess westward group and phase speeds. They showed that these long waves, presumably forced in the convective regions of the eastern Indian and western Pacific oceans (where $U(200 \text{ mb}) \ll 0$), would propagate into regions where $U_x < 0$. If the frequency of these modes is greater than that of the variation of the basic state, then (1) and (2) indicate that the mode must *decrease* its' longitudinal scale during westward propagation. Figure 15 shows how the Doppler shifted frequency approaches zero in the $U_x < 0$ region for such modes. Clearly, as k increases with westward propagation into the $U_x < 0$ region, C_{gd}^g decreases negatively. Somewhere near where $U_x < 0$ is a maximum. W&C show that $C_{gd}^g \rightarrow 0$.

W&C, at the time, did not consider the excitation of smaller scale modes which would initially possess positive group velocities so that $C_{gd}^g > 0$. Such modes would propagate eastwards into regions of increasing westerlies and where $U_x > 0$! Thus, from (1), k must decrease as it moves eastward and C_{gd}^g must increase negatively so that C_{gd}^g also goes to zero for these modes. The approach to zero of the Doppler-shifted group speed for the small scale case is also shown in Figure 9.

Figure 16 (Chang and Webster, 1989) shows a time-longitude plot along the equator of the perturbation zonal velocity component for the linear and nonlinear cases using a numerical model with an $U(x,y)$ basic state for the linear and nonlinear basic states. The bottom panel shows the difference fields. Note the similarity of the linear and nonlinear results. Figure 17 shows a sequence of the longitude-latitude plots of the divergence field. The Rossby waves are denoted as R_i and the Kelvin wave as K . The

latter mode propagates rapidly eastward with the basic state having little impact on its' characteristics. Two Rossby wave packets (R_1 and R_2 emerge from the region of excitation but in different directions. Both packets accumulate in the region of the westerlies. Respectively, they represent the backward and forward accumulation of the short- and long-wave Rossby packets.

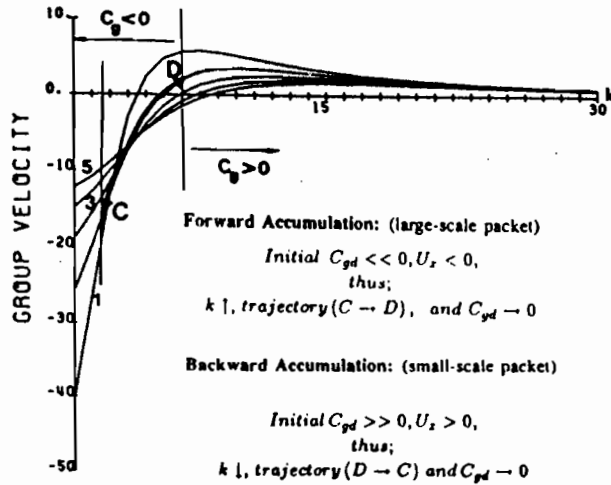


FIG.15. Plot of the group speed as a function of k for various n . As the scale changes subject to the laws (4) and (5), the group speed changes so that the Doppler group speed approaches a zero in the negative stretching deformation region. For the parameter range given by the low latitude basic state at low latitudes, all modes will accumulate at some point along the equator.

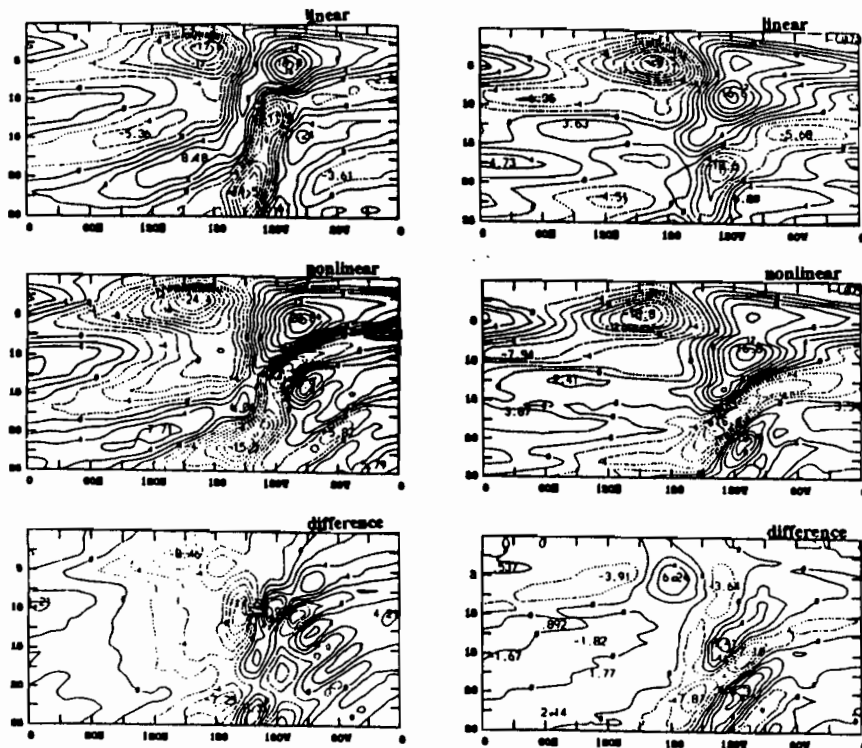


FIG.16. Time-longitude plots of the zonal velocity component around the equator of the linear (upper panels), nonlinear (middle) and the difference fields (bottom) for fluids of equivalent depths of 2000 m (left column) and 500 m (right column).

506
 $h = 500 \text{ m}$

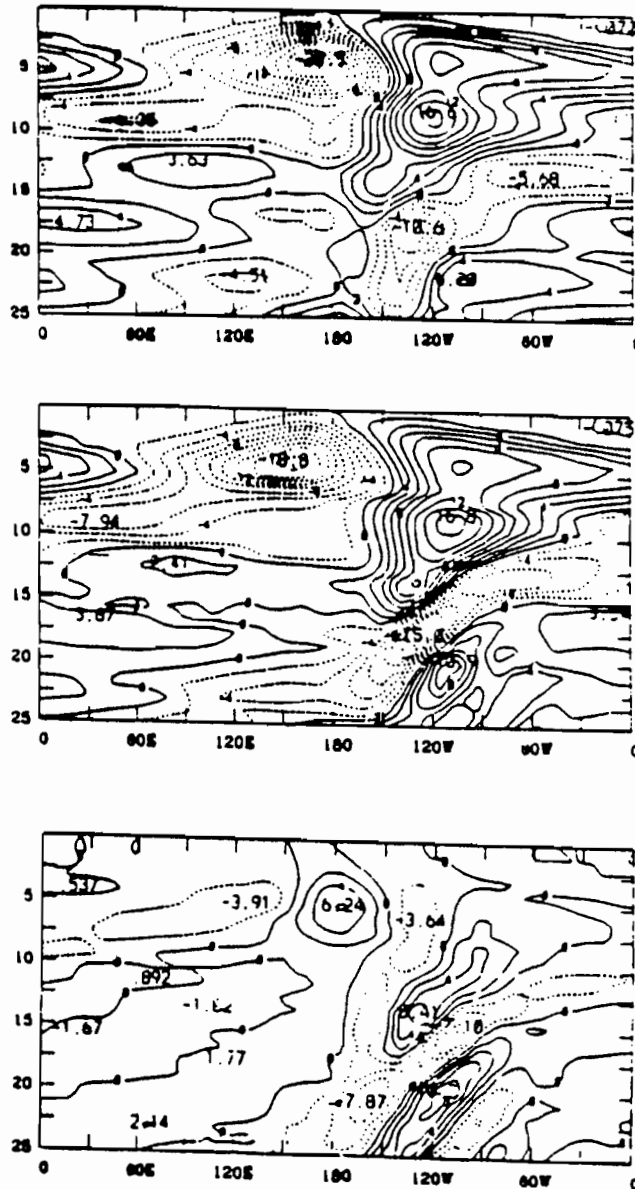


FIG.17. Time evolution of the divergence field for a 500 m fluid forced at location B in Fig. 6. Plots are shown at two day intervals for the first 23 days of integration. Lines indicate the characteristics of Rossby waves (R_1 , R_2 and R_3) and the Kelvin wave (K). Distinctions between the modes are made in the text.

In summary, for all equatorial Rossby modes, irrespective of their longitudinal scale, the equatorial westerlies act as a "wave attractor"; or as a general energy accumulation region. For reference, we refer to those modes that move westward to the accumulation region as "forward accumulation". The reverse, the eastward propagation and modification, we refer to as "backward accumulation". It turns out that it is very important to understand the difference in the form of the accumulation, especially when vertical propagation of the equatorial modes is considered.

e. Extensions (swelling) of equatorially trapped modes into the extratropics: An interpretation of the influence of tropical transients on higher latitudes:

In their numerical experiments, W&C noticed that, from the region of accumulation along the equator, and to the east of the equatorial westerlies (see Fig. 9), disturbances appear to emanate to higher latitudes. Similar results have been obtained from experiments using considerably more sophisticated models (Frederiksen and

Webster, 1987, and, Gelaro, personal communication). Although it appears that the accumulation region is acting as a Rossby wave-train source in the form of Hoskins and Karoly (1981), it does not appear as a likely explanation simply because the emanation exists in the linear model results as well as in the nonlinear calculations. Thus, if nonlinear interactions are not possible, there must be another explanation.

An explanation arises quite simply out of the W&C and Z&W results. Rather than a propagating mode being produced, it appears more likely that the influence at higher latitudes is being caused by the increase in the turning latitude of the equatorially trapped modes as they propagate into the equatorial westerlies. As a mode moves along the equator from regional easterlies to westerlies, the turning latitude will change with the change as shown in Figure 11. At the same time, at least for the westward propagating mode, the longitudinal scale will decrease due to the impact of the stretching deformation. The turning latitude-wavenumber trajectory as the mode moves to the west from easterlies to westerlies can be seen as the dashed line A-B in Figure 5. A schematic representation for both forward and backward modes is shown in Figure 18.

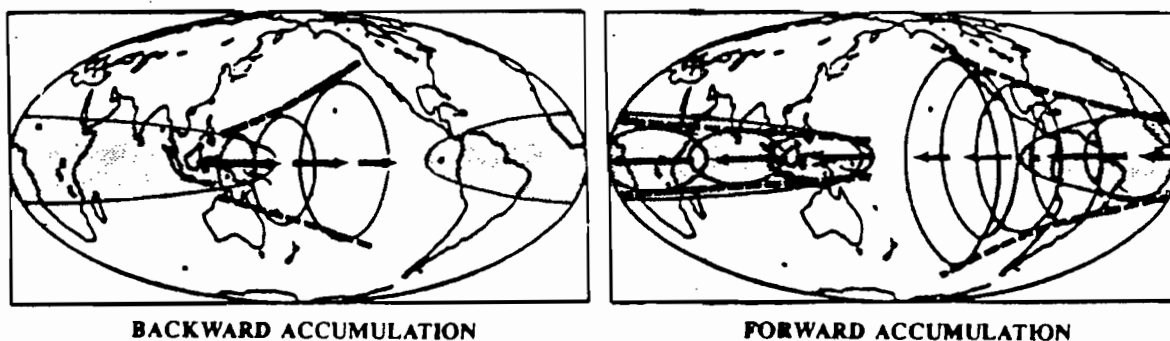


FIG.18. Schematic representation of "backward" (left panel) and "forward" (right panel) accumulation along the equator. Note, despite the direction of the initial propagation, the modes accumulate in the westerlies and "swell" to higher latitudes. The swelling is due to the increase of the turning latitude of the Rossby mode as it moves from the background easterlies to the westerlies.

f. Extratropical influences on the tropics:

The extensions of the equatorial modes to higher latitudes in the regions of the upper tropospheric equatorial westerlies has considerable impact on the interaction of extratropical transients on the tropics. The equatorial westerlies, of course, correspond to Webster and Holton's "westerly duct". Rather than extratropical modes merely propagating through the duct from one hemisphere to the other, as proposed by Webster and Holton, it is possible for extratropical forcing to produce a *trapped* equatorial response. There are two factors which determine the equatorial response to forcing. The longitudinal location of the forcing determines the proximity of the mode to the duct (see Webster and Holton). Given that the forcing is meridionally aligned with the duct, the latitudinal position relative to the turning latitude of an equatorially trapped mode is important. If the forcing is within the turning latitude (location Y poleward of the dashed line in Fig. 9), the forcing can project onto the trapped mode and an equatorially trapped response will be invoked. If the forcing is poleward of the turning latitude (location X, Fig. 9), a propagating mode (untrapped) will ensue. Figure 13 shows easterly and westerly basic flows forced by extratropical forcing. With the westerly turning latitudes that extend well poleward, an odd equatorial trapped mode is produced. In the easterly, where the turning latitudes are constrained near the equator, there is no equatorially trapped response.

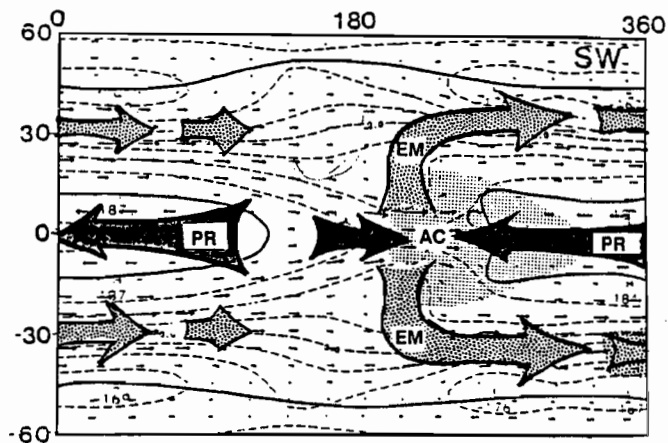


FIG.19. Schematic diagram showing the corridors of transmission of energy from the convective regions of the tropical warm pools to higher latitudes.

4. Conclusions.

It is clear that the basic flow invokes an extremely strong control on the form of the response to forcing from either tropical or extratropical sources. The control of the basic flow extends from the *in situ* response to the remote response and determines, to a great degree, how influence is manifested, in both directions, between the tropics and higher latitudes. In other words, to understand the interaction of the basic flow and the transients, it is necessary to take into account both the longitudinal and latitudinal variation of the basic flow and its' divergent characteristics. Finally, it would appear that much of the interaction can be understood in terms of the structure of equatorially trapped modes within varying basic flows and still be within the confines of equatorially trapped modes.

Within the framework of the theory outlined above, we can summarize the hypothesis of how transient waves, originating in the convectively active warm pools, transmit their influence to other regions of the tropics and the higher latitudes. Figure 19 provides a summary of the hypothesis. Waves propagate away from the source region in both directions along the equator. The large scale end of the wave packet propagates westward while the short scale end propagates eastward. Both trains accumulate in the negative stretching deformation region where they assume a greater latitudinal extent due to the scale modifications occurring in the westerly flow. In this manner, corridors through which energy passes from the convective zones to higher latitudes are created.

There are still a number of questions that remain unanswered. For example, the vertical propagation of the modes moving away from the convective source regions needs to be addressed. Also, we have not explicitly taken into account in our discussion the characteristics of the mixed Rossby-gravity mode. At larger scales, the mode possesses a relatively high frequency but asymptotes the lower Rossby wave frequency range at smaller scales. Zhang and Webster (1989) have shown that the mode is only moderately affected by the basic state. Thus, it presents the possibility of extending directly poleward from the point of excitation. Clearly, the role of the mixed Rossby-gravity mode deserves investigation.

REFERENCE

- Chang, H.-R. and P. J. Webster, 1989: Energy accumulation and emanation at low latitudes. Part II: Nonlinear response to strong episodic forcing. Submitted to *J. Atmos. Sci.*
- Charney, J. G., 1969: A further note on the large scale motions in the tropics. *J. Atmos. Sci.*, **34**, 901-910.
- Gill, A., 1980: Some simple solutions for heat induced tropical circulations. *Quart. J. Roy. Met. Soc.*, **106**, 447-462.
- Hoskins, B. J. and D. Karoly, 1981: The steady state response of a spherical atmosphere to thermal and orographic forcing, *J. Atmos. Sci.*, **38**, 1179-1196.
- Karoly, D., 1983: Rossby wave propagation in a barotropic atmosphere, *Dyn. Atmos. Oceans.*, **7**, 111-125.
- Longuet-Higgins, M. S., The eigenfunctions of Laplace's tidal equations, *Phil. Trans. R. Soc.*, **A262**, 511-607.
- Mak, M.-K.: Laterally driven stochastic motions in the tropics. *J. Atmos. Sci.*, **26**, 41-64.
- Matsuno, T., 1966: Quasi-geostrophic motions in the equatorial area, *J. Meteor. Soc. Japan*, **44**, 25-42.
- Nakazawa, T., 1988: Tropical super-clusters under intraseasonal variation, Japan-U.S. Workshop on the ENSO Phenomena, University of Tokyo, Nov. 3-7, 1987, Meteorological Research Report, #88-1, Department of Meteorology, Geophysical Institute, 76-78.
- Opsteegh, J. D., and H. M. Van den Dool, 1980: Seasonal differences in the stationary response of a linearized primitive equation model: Prospects for long-range forecasting? *J. Atmos. Sci.*, **37**, 2169-2185.
- Sardeshmukh, P. D. and B. J. Hoskins, 1988: The generation of global rotational flow by idealized tropical divergence. *J. Atmos. Sci.*, **45**, 1228-1251.
- Webster, P. J., 1971: Response of the tropical atmosphere to local steady forcing. *Mon. Wea. Rev.*, **100**, 518-540.
- Webster, P. J., 1973: Temporal variation of low latitude zonal circulations, *Mon. Wea. Rev.*, **101**, 803-816.
- Webster, P. J., 1981: Mechanisms determining the atmospheric response to sea surface temperature anomalies. *J. Atmos. Sci.*, **38**, 554-571.>
- Webster, P. J., 1982: Seasonality in the local and remote response to sea surface temperature anomalies, *J. Atmos. Sci.*, **39**, 41-42.
- Webster, P. J., 1983: Large scale structure of the tropical atmosphere. *Large-scale Dynamical Processes in the Atmosphere*, B. J. Hoskins and R. P. Pearce, Eds, Academic press, 392 pp.
- Webster P. J., and H.-R. Chang, 1988: Equatorial energy accumulation and emanation regions: Impacts of a zonally varying basic state, *J. Atmos. Sci.*, **45**, 803-829.
- Webster, P. J., and J. R. Holton, 1982: Cross equatorial response to mid-latitude forcing in a zonally varying basic state. *J. Atmos. Sci.*, **39**, 722-733.
- Zhang, C. and P. J. Webster, 1989: Effects of zonal flows on the equatorially trapped waves, to appear in *J. Atmos. Sci.*

**WESTERN PACIFIC INTERNATIONAL MEETING
AND WORKSHOP ON TOGA COARE**

Nouméa, New Caledonia

May 24-30, 1989

PROCEEDINGS

edited by

Joël Picaut *

Roger Lukas **

Thierry Delcroix *

* ORSTOM, Nouméa, New Caledonia

** JIMAR, University of Hawaii, U.S.A.

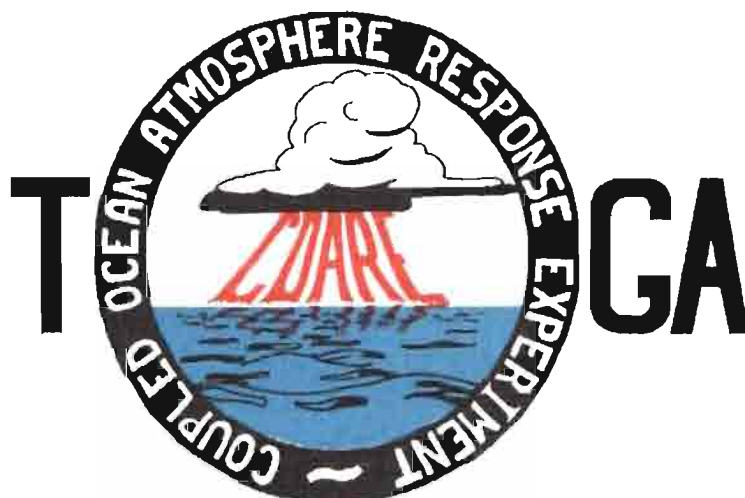


TABLE OF CONTENTS

ABSTRACT	i
RESUME	iii
ACKNOWLEDGMENTS	vi
INTRODUCTION	
1. Motivation	1
2. Structure	2
LIST OF PARTICIPANTS	5
AGENDA	7
WORKSHOP REPORT	
1. Introduction	19
2. Working group discussions, recommendations, and plans	20
a. Air-Sea Fluxes and Boundary Layer Processes	20
b. Regional Scale Atmospheric Circulation and Waves	24
c. Regional Scale Oceanic Circulation and Waves	30
3. Related programs	35
a. NASA Ocean Processes and Satellite Missions	35
b. Tropical Rainfall Measuring Mission	37
c. Typhoon Motion Program	39
d. World Ocean Circulation Experiment	39
4. Presentations on related technology	40
5. National reports	40
6. Meeting of the International Ad Hoc Committee on TOGA COARE	40
APPENDIX: WORKSHOP RELATED PAPERS	
Robert A. Weller and David S. Hosom: Improved Meteorological Measurements from Buoys and Ships for the World Ocean Circulation Experiment	45
Peter H. Hildebrand: Flux Measurement using Aircraft and Radars	57
Walter F. Dabberdt, Hale Cole, K. Gage, W. Ecklund and W.L. Smith: Determination of Boundary-Layer Fluxes with an Integrated Sounding System	81

MEETING COLLECTED PAPERS

WATER MASSES, SEA SURFACE TOPOGRAPHY, AND CIRCULATION

Klaus Wyrtki: Some Thoughts about the West Pacific Warm Pool	99
Jean René Donguy, Gary Meyers, and Eric Lindstrom: Comparison of the Results of two West Pacific Oceanographic Expeditions FOC (1971) and WEPOCS (1985-86)	111
Dunxin Hu, and Maochang Cui: The Western Boundary Current in the Far Western Pacific Ocean	123
Peter Hacker, Eric Firing, Roger Lukas, Philipp L. Richardson, and Curtis A. Collins: Observations of the Low-latitude Western Boundary Circulation in the Pacific during WEPOCS III	135
Stephen P. Murray, John Kindle, Dharma Arief, and Harley Hurlburt: Comparison of Observations and Numerical Model Results in the Indonesian Throughflow Region	145
Christian Henin: Thermohaline Structure Variability along 165°E in the Western Tropical Pacific Ocean (January 1984 - January 1989)	155
David J. Webb, and Brian A. King: Preliminary Results from Charles Darwin Cruise 34A in the Western Equatorial Pacific	165
Warren B. White, Nicholas Graham, and Chang-Kou Tai: Reflection of Annual Rossby Waves at The Maritime Western Boundary of the Tropical Pacific	173
William S. Kessler: Observations of Long Rossby Waves in the Northern Tropical Pacific	185
Eric Firing, and Jiang Songnian: Variable Currents in the Western Pacific Measured During the US/PRC Bilateral Air-Sea Interaction Program and WEPOCS	205
John S. Godfrey, and A. Weaver: Why are there Such Strong Steric Height Gradients off Western Australia ?	215
John M. Toole, R.C. Millard, Z. Wang, and S. Pu: Observations of the Pacific North Equatorial Current Bifurcation at the Philippine Coast	223

EL NINO/SOUTHERN OSCILLATION 1986-87

Gary Meyers, Rick Bailey, Eric Lindstrom, and Helen Phillips: Air/Sea Interaction in the Western Tropical Pacific Ocean during 1982/83 and 1986/87	229
Laury Miller, and Robert Cheney: GEOSAT Observations of Sea Level in the Tropical Pacific and Indian Oceans during the 1986-87 El Nino Event	247
Thierry Delcroix, Gérard Eldin, and Joël Picaut: GEOSAT Sea Level Anomalies in the Western Equatorial Pacific during the 1986-87 El Nino, Elucidated as Equatorial Kelvin and Rossby Waves	259
Gérard Eldin, and Thierry Delcroix: Vertical Thermal Structure Variability along 165°E during the 1986-87 ENSO Event	269
Michael J. McPhaden: On the Relationship between Winds and Upper Ocean Temperature Variability in the Western Equatorial Pacific	283

John S. Godfrey, K. Ridgway, Gary Meyers, and Rick Bailey: Sea Level and Thermal Response to the 1986-87 ENSO Event in the Far Western Pacific	291
Joël Picaut, Bruno Camusat, Thierry Delcroix, Michael J. McPhaden, and Antonio J. Busalacchi: Surface Equatorial Flow Anomalies in the Pacific Ocean during the 1986-87 ENSO using GEOSAT Altimeter Data	301

THEORETICAL AND MODELING STUDIES OF ENSO AND RELATED PROCESSES

Julian P. McCreary, Jr.: An Overview of Coupled Ocean-Atmosphere Models of El Nino and the Southern Oscillation	313
Kensuke Takeuchi: On Warm Rossby Waves and their Relations to ENSO Events	329
Yves du Penhoat, and Mark A. Cane: Effect of Low Latitude Western Boundary Gaps on the Reflection of Equatorial Motions	335
Harley Hurlburt, John Kindle, E. Joseph Metzger, and Alan Wallcraft: Results from a Global Ocean Model in the Western Tropical Pacific	343
John C. Kindle, Harley E. Hurlburt, and E. Joseph Metzger: On the Seasonal and Interannual Variability of the Pacific to Indian Ocean Throughflow	355
Antonio J. Busalacchi, Michael J. McPhaden, Joël Picaut, and Scott Springer: Uncertainties in Tropical Pacific Ocean Simulations: The Seasonal and Interannual Sea Level Response to Three Analyses of the Surface Wind Field	367
Stephen E. Zebiak: Intraseasonal Variability - A Critical Component of ENSO ?	379
Akimasa Sumi: Behavior of Convective Activity over the "Jovian-type" Aqua-Planet Experiments	389
Ka-Ming Lau: Dynamics of Multi-Scale Interactions Relevant to ENSO	397
Pecheng C. Chu and Roland W. Garwood, Jr.: Hydrological Effects on the Air-Ocean Coupled System	407
Sam F. Iacobellis, and Richard C.J. Somerville: A one Dimensional Coupled Air-Sea Model for Diagnostic Studies during TOGA-COARE	419
Allan J. Clarke: On the Reflection and Transmission of Low Frequency Energy at the Irregular Western Pacific Ocean Boundary - a Preliminary Report	423
Roland W. Garwood, Jr., Pecheng C. Chu, Peter Muller, and Niklas Schneider: Equatorial Entrainment Zone : the Diurnal Cycle	435
Peter R. Gent: A New Ocean GCM for Tropical Ocean and ENSO Studies	445
Wasito Hadi, and Nuraini: The Steady State Response of Indonesian Sea to a Steady Wind Field	451
Pedro Ripa: Instability Conditions and Energetics in the Equatorial Pacific	457
Lewis M. Rothstein: Mixed Layer Modelling in the Western Equatorial Pacific Ocean	465
Neville R. Smith: An Oceanic Subsurface Thermal Analysis Scheme with Objective Quality Control	475
Duane E. Stevens, Qi Hu, Graeme Stephens, and David Randall: The hydrological Cycle of the Intraseasonal Oscillation	485
Peter J. Webster, Hai-Ru Chang, and Chidong Zhang: Transmission Characteristics of the Dynamic Response to Episodic Forcing in the Warm Pool Regions of the Tropical Oceans	493

MOMENTUM, HEAT, AND MOISTURE FLUXES BETWEEN ATMOSPHERE AND OCEAN

W. Timothy Liu: An Overview of Bulk Parametrization and Remote Sensing of Latent Heat Flux in the Tropical Ocean	513
E. Frank Bradley, Peter A. Coppin, and John S. Godfrey: Measurements of Heat and Moisture Fluxes from the Western Tropical Pacific Ocean	523
Richard W. Reynolds, and Ants Leetmaa: Evaluation of NMC's Operational Surface Fluxes in the Tropical Pacific	535
Stanley P. Hayes, Michael J. McPhaden, John M. Wallace, and Joël Picaut: The Influence of Sea-Surface Temperature on Surface Wind in the Equatorial Pacific Ocean	543
T.D. Keenan, and Richard E. Carbone: A Preliminary Morphology of Precipitation Systems In Tropical Northern Australia	549
Phillip A. Arkin: Estimation of Large-Scale Oceanic Rainfall for TOGA	561
Catherine Gautier, and Robert Frouin: Surface Radiation Processes in the Tropical Pacific	571
Thierry Delcroix, and Christian Henin: Mechanisms of Subsurface Thermal Structure and Sea Surface Thermo-Haline Variabilities in the South Western Tropical Pacific during 1979-85 - A Preliminary Report	581
Greg. J. Holland, T.D. Keenan, and M.J. Manton: Observations from the Maritime Continent : Darwin, Australia	591
Roger Lukas: Observations of Air-Sea Interactions in the Western Pacific Warm Pool during WEPOCS	599
M. Nunez, and K. Michael: Satellite Derivation of Ocean-Atmosphere Heat Fluxes in a Tropical Environment	611

EMPIRICAL STUDIES OF ENSO AND SHORT-TERM CLIMATE VARIABILITY

Klaus M. Weickmann: Convection and Circulation Anomalies over the Oceanic Warm Pool during 1981-1982	623
Claire Perigaud: Instability Waves in the Tropical Pacific Observed with GEOSAT	637
Ryuichi Kawamura: Intraseasonal and Interannual Modes of Atmosphere-Ocean System Over the Tropical Western Pacific	649
David Gutzler, and Tamara M. Wood: Observed Structure of Convective Anomalies	659
Siri Jodha Khalsa: Remote Sensing of Atmospheric Thermodynamics in the Tropics	665
Bingrong Xu: Some Features of the Western Tropical Pacific: Surface Wind Field and its Influence on the Upper Ocean Thermal Structure	677
Bret A. Mullan: Influence of Southern Oscillation on New Zealand Weather	687
Kenneth S. Gage, Ben Basley, Warner Ecklund, D.A. Carter, and John R. McAfee: Wind Profiler Related Research in the Tropical Pacific	699
John Joseph Bates: Signature of a West Wind Convective Event in SSM/I Data	711
David S. Gutzler: Seasonal and Interannual Variability of the Madden-Julian Oscillation	723
Marie-Hélène Radenac: Fine Structure Variability in the Equatorial Western Pacific Ocean	735
George C. Reid, Kenneth S. Gage, and John R. McAfee: The Climatology of the Western Tropical Pacific: Analysis of the Radiosonde Data Base	741

Chung-Hsiung Sui, and Ka-Ming Lau: Multi-Scale Processes in the Equatorial Western Pacific	747
Stephen E. Zebiak: Diagnostic Studies of Pacific Surface Winds	757

MISCELLANEOUS

Rick J. Bailey, Helene E. Phillips, and Gary Meyers: Relevance to TOGA of Systematic XBT Errors	775
Jean Blanchot, Robert Le Borgne, Aubert Le Bouteiller, and Martine Rodier: ENSO Events and Consequences on Nutrient, Planktonic Biomass, and Production in the Western Tropical Pacific Ocean	785
Yves Dandonneau: Abnormal Bloom of Phytoplankton around 10°N in the Western Pacific during the 1982-83 ENSO	791
Cécile Dupouy: Sea Surface Chlorophyll Concentration in the South Western Tropical Pacific, as seen from NIMBUS Coastal Zone Color Scanner from 1979 to 1984 (New Caledonia and Vanuatu)	803
Michael Szabados, and Darren Wright: Field Evaluation of Real-Time XBT Systems	811
Pierre Rual: For a Better XBT Bathy-Message: Onboard Quality Control, plus a New Data Reduction Method	823